Solubility of the metal precursor Ni(NO3)2·6H2O in high-pressure CO2 + ethanol mixtures

Journal:	*Journal of Chemical & Engineering Data*
Manuscript ID	je-2017-00804a.R1
Manuscript Type:	Article
Date Submitted by the Author:	01-Nov-2017
Complete List of Authors:	Tenorio, María; Universidad Complutense de Madrid, Departamento de Química Física I Ginés, Sonia; Universidad Complutense de Madrid Pando, Concepción; Universidad Complutense de Madrid, Quimica Fisica I Renuncio, Juan; Universidad Complutense, Departamento Quimica Fisica I Cabañas, Albertina; Universidad Complutense, Química-Física I

Solubility of the metal precursor $Ni(NO_3)_2 \cdot 6H_2O$ in high-pressure CO_2 + ethanol mixtures

María José Tenorio, Sonia Ginés, Concepción Pando, Juan Antonio R. Renuncio and Albertina Cabañas*

Departamento de Química–Física I, Universidad Complutense de Madrid, 28040 Madrid, SPAIN.

*Send correspondence to:
Prof. Albertina Cabañas
Departamento de Química-Física I
UNIVERSIDAD COMPLUTENSE DE MADRID
Ciudad Universitaria s/n, 28040 Madrid, SPAIN.
Tlf: 34 + 91 394 5225
Fax: 34 + 91 394 4135
e-mail: a.cabanas@quim.ucm.es

Abstract

The solubility of $Ni(NO_3)_2 \cdot 6H_2O$ in high-pressure CO_2 + ethanol mixtures was measured using a high-pressure variable-volume view cell from (308.2 to 353.2 K) and up to 25.0 MPa. This compound has been used previously as a Ni precursor in metal deposition experiments using supercritical CO_2. $Ni(NO_3)_2 \cdot 6H_2O$ was not soluble in pure CO_2 but the addition of ethanol into the system allowed the solubilisation of the hydrated salt in the mixture. Mole fraction of $Ni(NO_3)_2 \cdot 6H_2O$ varied from $1.67\ 10^{-4}$ to $1.97\ 10^{-3}$. At these salt concentrations, the phase diagram of the CO_2 + EtOH + $Ni(NO_3)_2 \cdot 6H_2O$ system resembled that of the CO_2 + EtOH binary system and, at the studied conditions, a vapour-liquid equilibrium was observed. For the higher ethanol concentrations, the bubble points closely matched those of the CO_2 + EtOH system. For the lower EtOH concentrations, however, much higher solubilisation pressures were required, due to the release of water molecules from the salt into the solution. $Ni(NO_3)_2 \cdot 6H_2O$ solutions were stable in high-pressure CO_2 + EtOH mixtures at the studied conditions.

Keywords: Supercritical Carbon Dioxide, Solubility, Hydrated Metal Salts, Ethanol, Modifier, CO_2-Expanded Liquids.

1. Introduction

The use of supercritical fluids and in particular supercritical CO_2 ($scCO_2$) to replace the more toxic organic solvents in environmentally benign processes is of increasing interest nowadays. CO_2 is cheap, non-toxic, non-flammable and has moderate critical parameters (T_c = 304.2 K, P_c = 7.4 MPa), therefore it is considered a green solvent.[1]

Knowledge of the high-pressure phase behaviour is essential in any application using $scCO_2$. Prof. Cor Peters has successfully contributed throughout the years to the study and understanding of the thermodynamic properties of high-pressure systems and has also played a key role in the development of innovative high-pressure applications. His outstanding contribution involved the formation of many students and postdoctoral researchers. Other colleagues such as ourselves also benefited from his talks and from discussions in conferences and courses.[2] C.P., J.A.R.R. and A.C. have enjoyed Cor Peters warm friendship for many years; it is an honour for us to participate in this issue celebrating his achievements.

High-pressure vapour-liquid equilibrium (VLE) measurements of CO_2 and alcohol systems are of interest due to their importance in the supercritical extraction of labile compounds, dehydration of alcohols using supercritical carbon dioxide and extraction of natural compounds.[3] Supercritical CO_2 as well as many other non-polar fluids are not good solvents for polar solutes. A small amount of a cosolvent or modifier is added to the fluid in order to improve its solvation power.[4] Alcohols, such as methanol or ethanol are often used to increase CO_2 polarity. If the amount of alcohol added is large enough, the system behaves such as an expanded liquid systems[5] and keeps most of the solvation power of the

liquid solvent. Therefore, mixtures of CO_2 and methanol or ethanol can dissolve more polar compounds.

One process that can benefit from the use of high pressure CO_2 + ethanol mixtures is the deposition of metal and metal oxides on inorganic and polymeric supports using supercritical fluids.[6, 7] The Supercritical Fluid Deposition (SCFD) technique involves the dissolution of a metal precursor in supercritical fluid, usually CO_2, and its adsorption onto the support. The metal precursor is then chemically or thermally decomposed on the support. The decomposition can be carried out after the depressurization or at supercritical conditions. Alcohols can also help in the reduction process.[8] Varying the experimental conditions, metal nanoparticles,[9] nanowires[10] or continuous supported films[11] have been produced. This technique offers many opportunities in the preparation of heterogeneous catalysts, ceramics, gas sensors and microelectronics, among others.

In our group, we have extensively investigated the deposition of Pd, Ru, Ni, Pt nanoparticles (NPs) on different inorganic supports.[12-16] The excellent catalytic properties of some of the materials produced were proved.[14, 16, 17] The method was also used to insert Ni nanoparticles into the pores of nanopatterned $BaTiO_3$ thin films for the preparation of multiferroics.[12]

Organometallic precursors are the metal precursor commonly used, because of their high solubility in supercritical CO_2.[18] However, these compounds are generally expensive, toxic (due to their high volatility) and oftentimes difficult to manipulate as they can be light and/or air sensitive. In contrast, inorganic polar precursors such as metal nitrates and chlorides do not have some of these problems, being the most popular metal precursors used in the preparation of metal oxides and metallic materials by conventional techniques.

Metal nitrates and chlorides tend to form hydrates, which are not soluble in $scCO_2$ but are soluble in methanol or ethanol. These alcohols are highly miscible with CO_2 at moderate conditions. In this case, the solubilisation of hydrated metal nitrates or chlorides can be accomplished by adding a small amount of the alcohol to supercritical CO_2 which acts as a cosolvent or by using a CO_2-expanded solution of the precursor in the alcohol. The use of metal nitrates and metal chlorides dissolved in high-pressure CO_2 + alcohol mixtures has been extensively studied by Profs. Z. Liu and B. Han at Beijing National Laboratory (China).[19, 20] In our group, we have also used this approach to deposit Ru and Ni NPs on different substrates.[12, 13, 16] The transport properties of the hydrated metal salts in the CO_2 alcohol mixtures are highly favoured in comparison to those of the metal salt solutions in pure alcohol. Nevertheless, apart from the report by Ming et al. [21] on the reaction of hydrous inorganic metal salts in CO_2-expanded ethanol, the phase behaviour of these systems has not been previously studied. Furthermore, no quantitative measurements of these systems have been performed.

In this paper, we study the phase behaviour of the mixtures formed by $Ni(NO_3)_2{\cdot}6H_2O$ in high pressure CO_2 + ethanol mixtures using a high-pressure variable volume view cell. Phase behaviour measurements are reported from (308.2 to 353.2 K). These data are compared to VLE data for the CO_2 + ethanol and CO_2 + ethanol + H_2O systems available in the literature.

2. Experimental

2.1 Materials. The details of the reagents used in this work are given in table 1. These materials were used as received.

Table 1 Specifications of the chemicals used in this work.

Chemical Name	Linear formula	CAS No.	Mw (g/mol)	Purity	Source
Carbon dioxide	CO_2	124-38-9	44.01	>99.99	Air Liquide
Nickel(II) nitrate hexahydrate	$Ni(NO_3)_2 \cdot 6H_2O$	13478-00-7	290.79	99.999	Sigma-Aldrich
Ethanol	C_2H_6O	64-17-5	46.07	>99.99	Fisher

2.2. Apparatus and Procedures. Equilibrium measurements of $Ni(NO_3)_2 \cdot 6H_2O$ in CO_2 + ethanol mixtures were carried out using a high-pressure variable volume view cell built and designed at our laboratory, following the procedure previously described.[22, 23] Figure 1 shows a schematic design of the view cell and images of $Ni(NO_3)_2 \cdot 6H_2O$ + EtOH and CO_2 + EtOH + $Ni(NO_3)_2 \cdot 6H_2O$ solutions. The cell is a stainless steel high-pressure cylinder fitted with a sapphire window in one side. The volume of the cell is varied by moving a stainless steel piston placed on the opposite side, the maximum working volume being 15 cm^3. The contents in the cell are illuminated and observed through the window using a Fiegert Endotech boroscope and a digital camera connected to a computer. The cell can be heated to 373 K using a silicone heating tape wrapped around the cylinder (Omegalux SRT051-040) connected to a Proportional Integral Derivative (PID) temperature controller (Microomega, model CN77322). A type J calibrated thermocouple inside the cell is used both as a control point and for measuring the temperature. The precision of the thermocouple is ±0.05 K and the stability of the thermostat during measurements is estimated to be ±0.2 K. The sample can be compressed (up to 30 MPa) or

decompressed by displacing the piston using a manual high pressure generator and water as hydrostatic fluid. The pressure is measured inside the cell using a relative transducer (Druck, model PTX7511-1) with an estimated error of ±(0.01 + 0.0015 P) MPa. This equipment has been previously used to measure the solubility of different Ni and Ru metal organic compounds in CO_2, both pure and modified with ethanol.[24, 25]

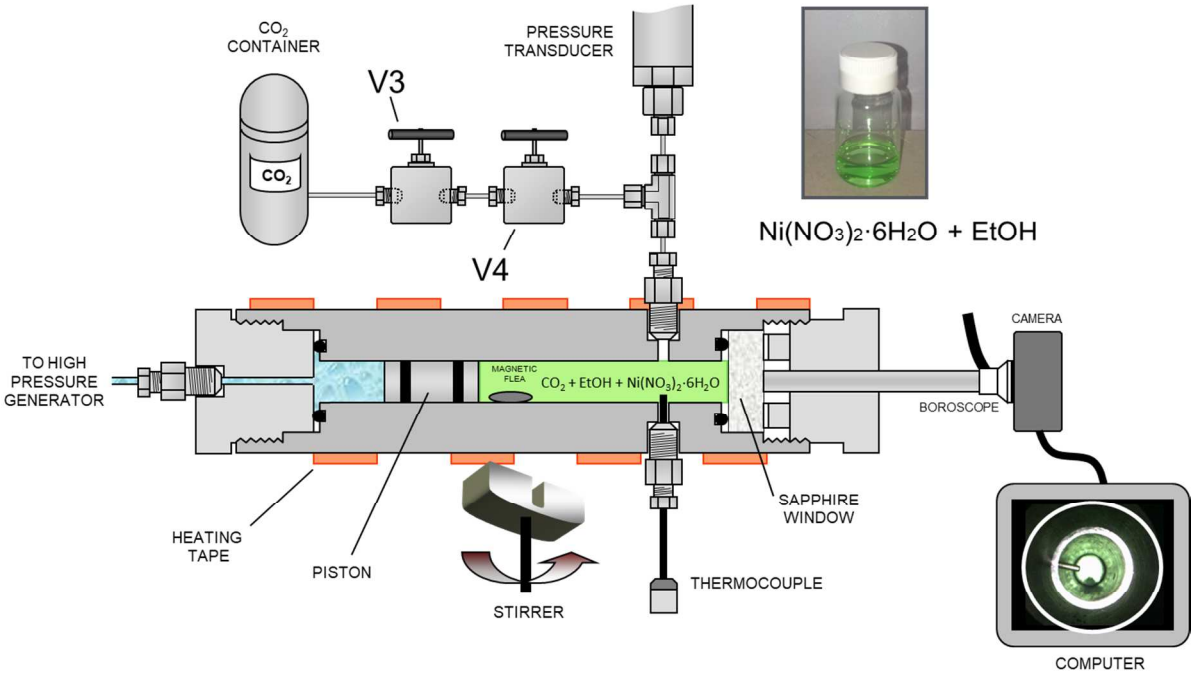

Figure 1. High pressure variable volume view cell and images of $Ni(NO_3)_2 \cdot 6H_2O$ + EtOH and CO_2 + EtOH + $Ni(NO_3)_2 \cdot 6H_2O$ solutions.

Solubility data were measured following the synthetic method by preparing a mixture of known composition and studying its phase behavior against pressure and temperature. Approximately 0.2 g of $Ni(NO_3)_2 \cdot 6H_2O$ was dissolved in 1.6 g of ethanol (2.0 cm^3). From this solution, between 0.5 to 0.9 g was loaded into the cell using a syringe. For the measurements at high ethanol concentrations, an extra volume of pure ethanol was introduced into the cell. The concentration of the solution and the amount loaded into the

cell were determined by weight using an analytical balance AND GR – 200 with a precision of ±0.001 g. Finally, liquid carbon dioxide was gravimetrically transferred into the cell by means of an auxiliary cell. Considering the precision of the weight measurements, the overall composition can be determined with an estimated error of 0.1%. Once the sample was loaded, the cell was kept at constant temperature and the sample was compressed to a single phase. The contents of the cell were agitated by a magnetic stirrer in order to assure homogeneity in the single phase. The pressure was then slowly decreased until the apparition of the second phase. Depending on the region of the phase diagram, the second phase appeared as a liquid phase (dew point) or a vapour phase (bubble point). The determination of this point was based on visual observation. At the studied compositions, no solid phase was observed. This process was reversed: the sample was pressurized to the homogeneous single phase and depressurized to the two-phase region repeatedly in order to get a precise pressure value for the pressure phase separation. Reproducibility in the pressure measurement was ±0.1 MPa.

$Ni(NO_3)_2 \cdot 6H_2O$ contains a large amount of crystallization water, which is released into the ethanol upon dissolution. In fact, the presence of water helps to dissolve the salt in the alcohol, which is required to be miscible with CO_2. To further assess the role that the water molecules play in the system, a particular solution of $Ni(NO_3)_2 \cdot 6H_2O$ in ethanol was dried using molecular sieves and mixed with CO_2. Molecular sieves (0.3 nm beads supplied by Merck) were activated in a conventional oven at 353 K for 24 hours. A given amount of molecular sieves following the manufacturer instructions was introduced into the solution and after 3 hours the solution was filtered and loaded into the cell following the procedure previously described. Phase behaviour measurements of the dried solution were performed.

3. Results and discussions

$Ni(NO_3)_2 \cdot 6H_2O$ was not soluble in pure CO_2 but the addition of ethanol into the system allowed the solubilisation of the hydrated salt in the mixture. $Ni(NO_3)_2 \cdot 6H_2O$ solutions of different ethanol concentration were used to cover a large ethanol concentration range. CO_2 mole fraction varied from 0.352 to 0.970, whilst ethanol mole fraction varied from 0.029 to 0.647. $Ni(NO_3)_2 \cdot 6H_2O$ mole fraction varied from $1.67\ 10^{-4}$ to $1.97\ 10^{-3}$ depending on the ethanol concentration.

$Ni(NO_3)_2 \cdot 6H_2O$ dissolved in ethanol and released the six crystallization water molecules into the medium. Upon addition of CO_2, the system could be considered as a quaternary system formed by CO_2, ethanol, H_2O, and $Ni(NO_3)_2$. The amount of water released into the system was estimated from the $Ni(NO_3)_2 \cdot 6H_2O$ concentration of the solution.

Solubility measurements were carried out at 308.2, 313.2, 323.2, 333.2, 343.2, and 353.2 K in the (5.2-25.0 MPa) pressure range. $Ni(NO_3)_2 \cdot 6H_2O$ solutions were stable at the studied conditions. The higher temperature used in this study, 353.2 K, is much lower than the decomposition temperature of 423 K previously reported for this salt in CO_2-expanded liquid systems.[21]

Solubility data of $Ni(NO_3)_2 \cdot 6H_2O$ in $scCO_2$ modified with ethanol at the different conditions are given in Table 2. Figures 2-7 show the phase diagram of $Ni(NO_3)_2 \cdot 6H_2O$ in

mixtures of CO_2 + EtOH at the different temperatures and compare these data to those of the CO_2 + EtOH binary system previously reported at the same temperature.

Table 2. Solubilisation conditions for the different solutions of $Ni(NO_3)_2 \cdot 6H_2O$ in CO_2 + EtOH mixtures at high pressure and temperatures from 308.2 to 353.2 K.[a]

			P / MPa						
x CO_2	*x* EtOH	*x* $Ni(NO_3)_2 \cdot 6H_2O$	308.2 K	313.2 K	323.2 K	333.2 K	343.2 K	353.2 K	Obs.[c]
0.352	0.647	$1.97\ 10^{-3}$	5.2	5.6	6.2	7.0	7.9	8.7	BP
0.438	0.561	$1.76\ 10^{-3}$	5.9	6.5	7.6	8.8	10.0	10.9	BP
0.486	0.513	$1.33\ 10^{-3}$	6.3	6.8	7.8	9.1	10.5	11.5	BP
0.526	0.473	$1.43\ 10^{-3}$	6.5	7.2	8.4	9.6	10.7	11.7	BP
0.586	0.414	$1.35\ 10^{-3}$	6.5	7.2	8.2	9.4	10.7	11.7	BP
0.608	0.391	$1.56\ 10^{-3}$	6.6	7.1	8.2	9.6	10.8	11.8	BP
0.655	0.344	$1.25\ 10^{-3}$	6.7	7.7	8.9	10.4	11.7	12.9	BP
0.668	0.331	$1.25\ 10^{-3}$	6.9	7.6	8.8	10.4	11.8	12.9	BP
0.709	0.290	$1.24\ 10^{-3}$	6.8	7.8	9.2	10.4	11.8	13.0	BP
0.759	0.240	$1.33\ 10^{-3}$	7.0	7.8	9.3	10.8	12.2	13.5	BP
0.813	0.185	$1.47\ 10^{-3}$	7.1	7.8	9.4	10.9	12.4	13.7	BP
0.839	0.160	$1.18\ 10^{-3}$	7.3	8.2	10.1	11.9	13.5	14.9	BP
0.937	0.062	$1.17\ 10^{-3}$	-	-	-	16.0	18.0	21.8	DP
0.945[b]	0.054	$1.15\ 10^{-3}$	-	7.8	8.9	10.4	11.7	12.9	DP
0.949	0.051	$1.51\ 10^{-3}$	7.7	9.0	12.0	13.8	-	17.3	DP
0.954	0.046	$1.67\ 10^{-4}$	7.8	11.5	14.1	15.8	-	19.1	DP
0.970	0.029	$3.79\ 10^{-4}$	7.7	8.9	11.4	13.0	-	14.8	DP

[a] Standard uncertainties *u* are $u(T)$/K = 0.2 , $u(P)$/MPa = 0.1, $u(x)$ = 0.1%.[b] Sample prepared using molecular sieves. [c] A bubble point (BP) or a dew point (DP) was observed.

Solubilisation pressures for the composition *x* CO_2 = 0.937, *x* EtOH = 0.062 and *x* $Ni(NO_3)_2 \cdot 6H_2O$ = $1.17\ 10^{-3}$ at 308.2, 313.2 and 323.2 K were not measured due to the very slow solubilisation process. At the higher temperatures, solubilisation was much faster. For the higher CO_2 compositions phase equilibrium measurements at 343.2 K were also omitted.

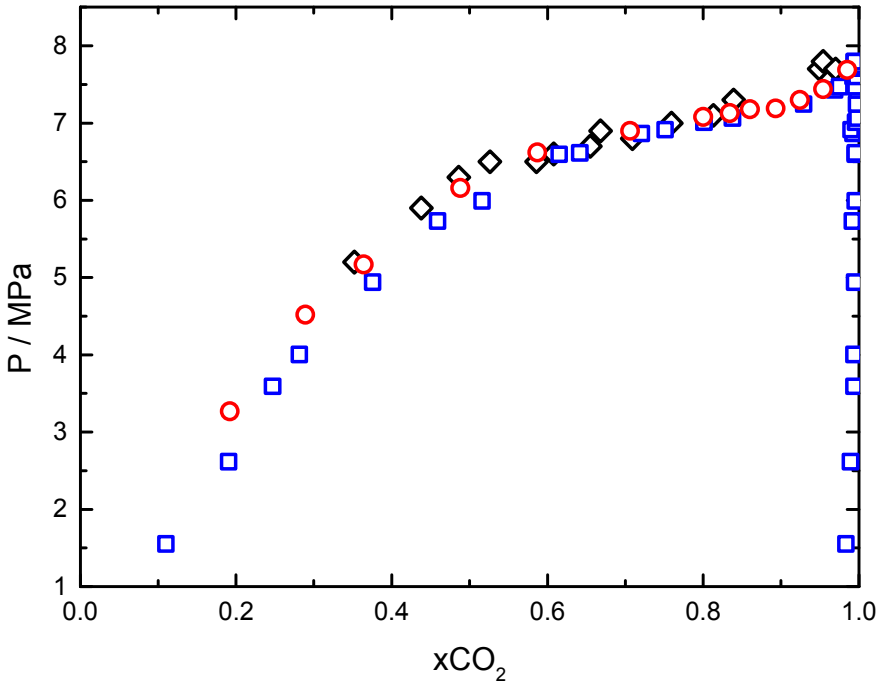

Figure 2. Phase diagram of the CO_2 + EtOH + $Ni(NO_3)_2 \cdot 6H_2O$ system at 308.2 K plotted as function of CO_2 mole fraction (◇) and comparison with the phase diagram of the binary system CO_2 + EtOH at the same temperature:(○) Chin *et al.* [26] and (□) Tanaka *et al.* [27]. $Ni(NO_3)_2 \cdot 6H_2O$ mole fraction values vary from 1.67 10^{-4} to 1.97 10^{-3} and are given in Table 2.

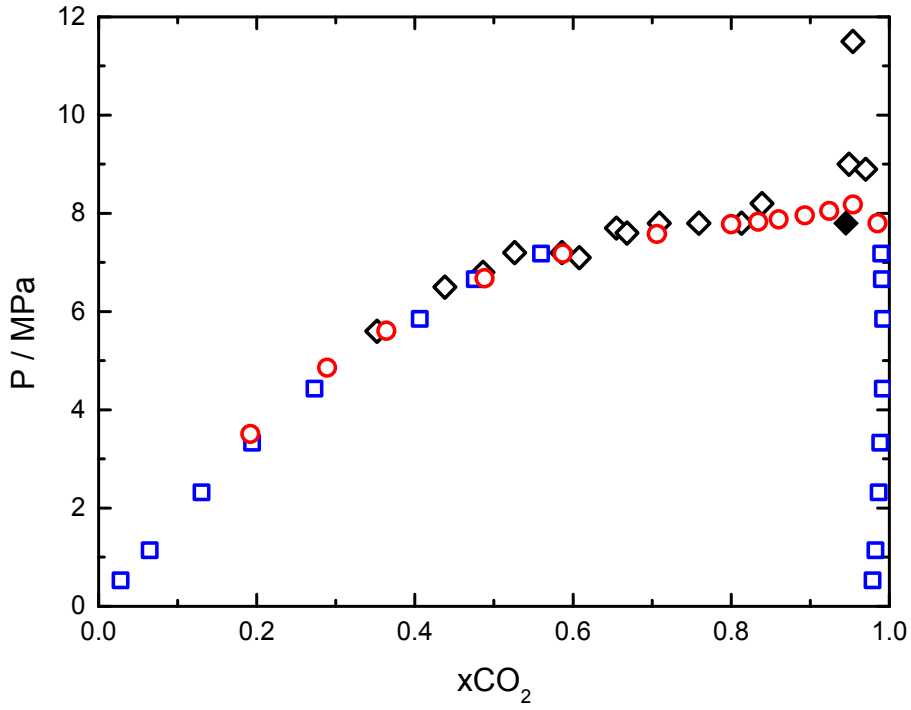

Figure 3. Phase diagram of the CO_2 + EtOH + $Ni(NO_3)_2 \cdot 6H_2O$ system at 313.2 K plotted as function of CO_2 mole fraction (◇) and comparison with the phase diagram of the binary system CO_2 + EtOH at the same temperature:(○) Chin *et al.* [26] and (□) Secuianu *et al.* [27]. (◆) Solution prepared adding molecular sieves. $Ni(NO_3)_2 \cdot 6H_2O$ mole fraction values vary from 1.67 10^{-4} to 1.97 10^{-3} and are given in Table 2.

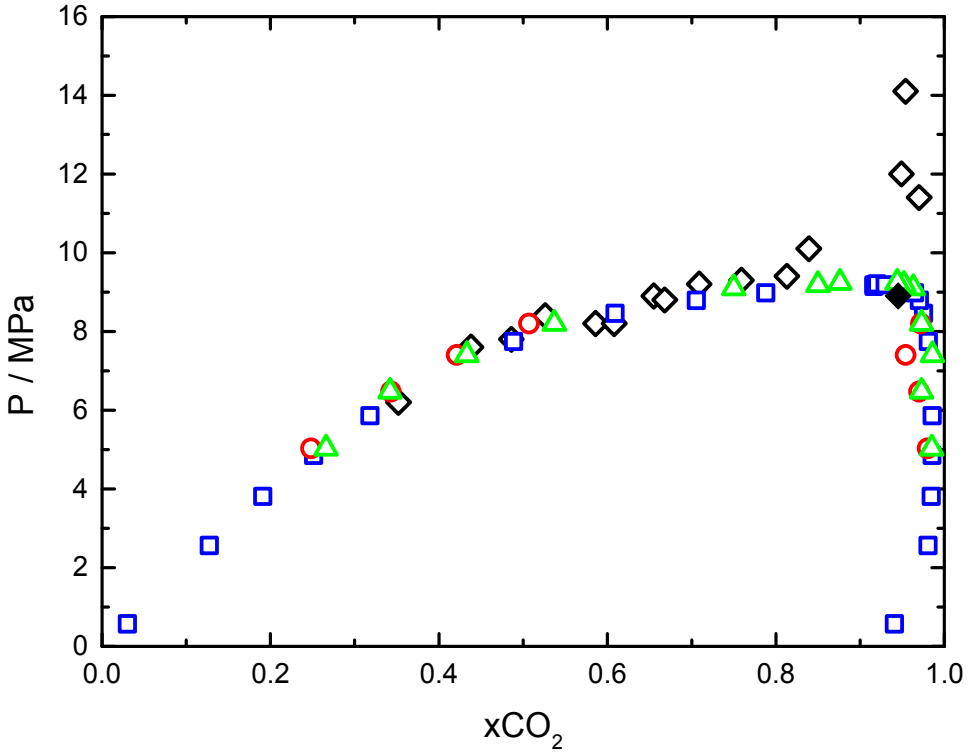

Figure 4. Phase diagram of the CO_2 + EtOH + $Ni(NO_3)_2 \cdot 6H_2O$ system at 323.2 K plotted as function of CO_2 mole fraction (◇) and comparison with the phase diagram of the binary system CO_2 + EtOH at the same temperature:(○) Chen *et al.* [28], (□) Joung *et al.* [29] and (△) Suzuki *et al.* [30].(◆) Solution prepared adding molecular sieves. $Ni(NO_3)_2 \cdot 6H_2O$ mole fraction values vary from 1.67 10^{-4} to 1.97 10^{-3} and are given in Table 2.

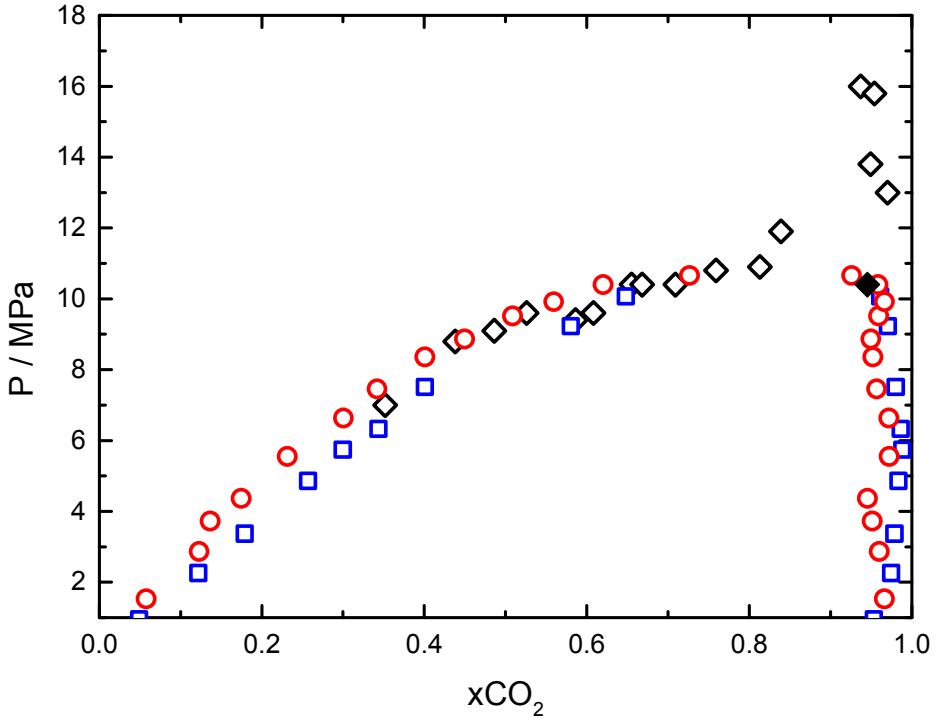

Figure 5. Phase diagram of the CO_2 + EtOH + $Ni(NO_3)_2 \cdot 6H_2O$ system at 333.2 K plotted as function of CO_2 mole fraction (◇) and comparison with the phase diagram of the binary system CO_2 + EtOH at the same temperature:(○) Knez *et al.* [31] and (□) Secuinanu *et al.* [32]. (◆) Solution prepared adding molecular sieves. $Ni(NO_3)_2 \cdot 6H_2O$ mole fraction values vary from 1.67 10^{-4} to 1.97 10^{-3} and are given in Table 2.

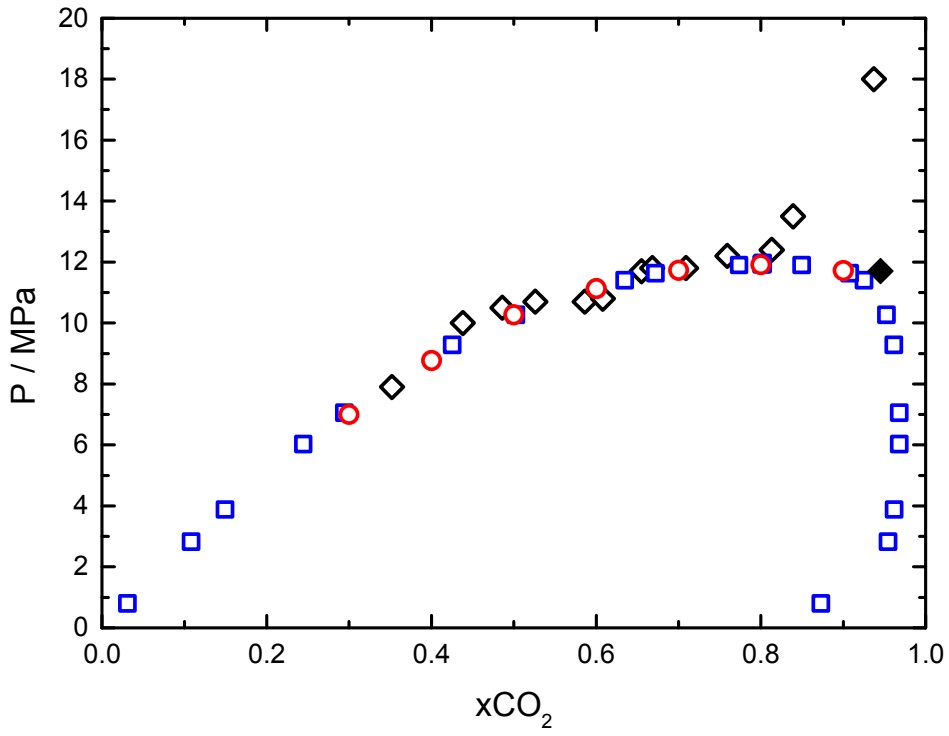

Figure 6. Phase diagram of the system CO_2 + EtOH + $Ni(NO_3)_2 \cdot 6H_2O$ system at 343.2 K plotted as function of CO_2 mole fraction (◇) and comparison with the phase diagram of the binary system CO_2 + EtOH at the same temperature:(○) Wu *et al.* [33] and (□) Joung *et al.* [29]. (◆) Solution prepared adding molecular sieves. $Ni(NO_3)_2 \cdot 6H_2O$ mole fraction values vary from 1.67 10^{-4} to 1.97 10^{-3} and are given in Table 2.

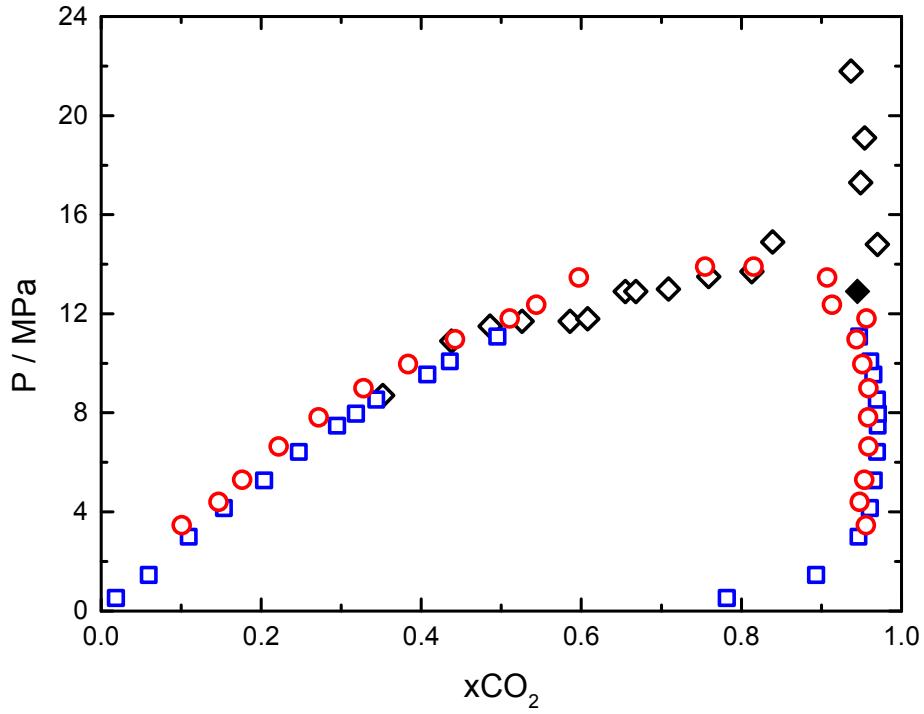

Figure 7. Phase diagram of the system CO_2 + EtOH + $Ni(NO_3)_2 \cdot 6H_2O$ system at 353.2 K plotted as function of CO_2 mole fraction (◇) and comparison with the phase diagram of the binary system CO_2 + EtOH at the same temperature:(○) Wu *et al.* [33], (□) Secuianu *et al.* [32] and (△) Knez *et al.* [31]. (◆) Solution prepared adding molecular sieves. $Ni(NO_3)_2 \cdot 6H_2O$ mole fraction values vary from 1.67 10^{-4} to 1.97 10^{-3} and are given in Table 2.

At high pressure, the system studied either formed one single phase or split upon depressurization into a vapour and a liquid phase in equilibrium showing the behaviour of a bubble or a dew point, depending on concentration, pressure and temperature.

Figure 8a shows a schematic representation of the CO_2 + EtOH binary phase diagram above the critical point of CO_2. Bubble and dew points merge in the critical point. Due to

the small concentration of $Ni(NO_3)_2 \cdot 6H_2O$ in comparison to those of CO_2 and EtOH, a similar behaviour was observed for the CO_2 + EtOH + $Ni(NO_3)_2 \cdot 6H_2O$ system. In the same figure, images of the view cell in a typical experiment show (b) two phases at low pressure, (c) one phase at higher pressure, and (d) a bubble and (e) a dew point upon depressurization.

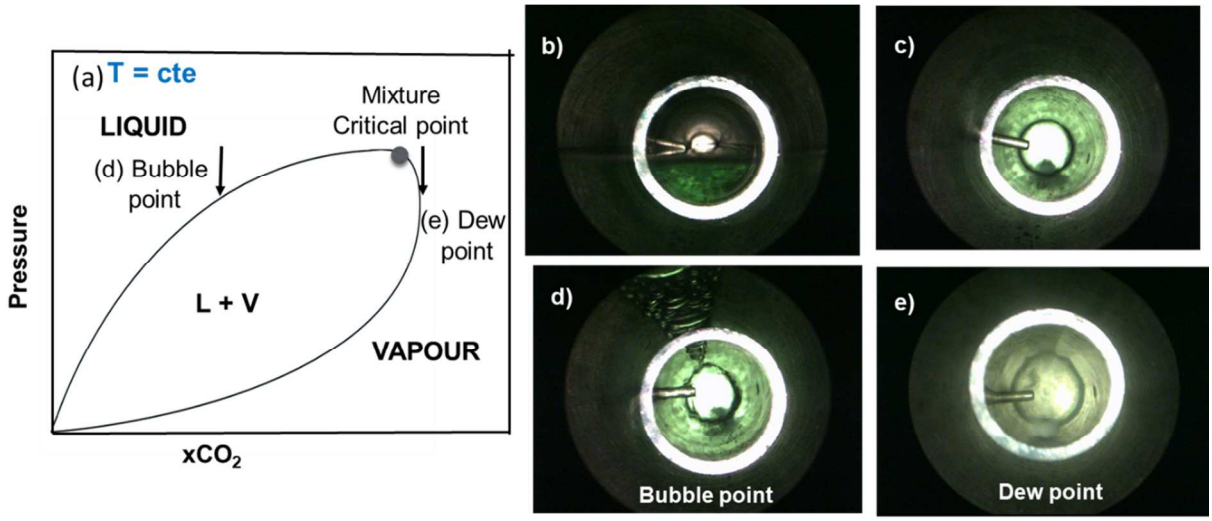

Figure 8. (a) Schematic representation of the CO_2 + EtOH binary phase diagram at a temperature above the critical temperature of CO_2. Images taken from the view cell in a typical CO_2 + EtOH + $Ni(NO_3)_2 \cdot 6H_2O$ experiment show: (b) two phases at low pressure, (c) one phase at higher pressure, (d) a bubble point and (e) a dew point.

At large EtOH concentrations, bubble points were observed at every temperature. The pressure conditions were very similar to those of the binary CO_2 + EtOH system, due to the low concentration of the salt into the system. At these conditions in the one-phase region, the system behaved as a CO_2-expanded liquid mixture rather than as a supercritical fluid mixture.

At much lower ethanol concentrations, however, the system behaved differently and, at every temperature, large deviations from the binary system were observed. Differences were much larger at the higher temperatures. Figure 9 shows images of the contents of the

cell in an experiment with CO_2 + EtOH + $Ni(NO_3)_2 \cdot 6H_2O$ at very low EtOH concentration. The composition of the mixture was: x CO_2= 0.941, x EtOH= 0.057, x $Ni(NO_3)_2 \cdot 6H_2O$ = 1.16 10^{-3}. The upper phase was rich in CO_2 and EtOH and exhibited a very mild green colour whilst the lower one, which was darker green coloured, was rich in H_2O and $Ni(NO_3)_2$. For this composition, the system did not form a single phase even at 353.2 K and 25.0 MPa. The system was not pressurized further to avoid breaking of the O-rings at high temperature. This pressure is much larger than that required to get single phase conditions in the CO_2 +EtOH binary system at a similar composition.

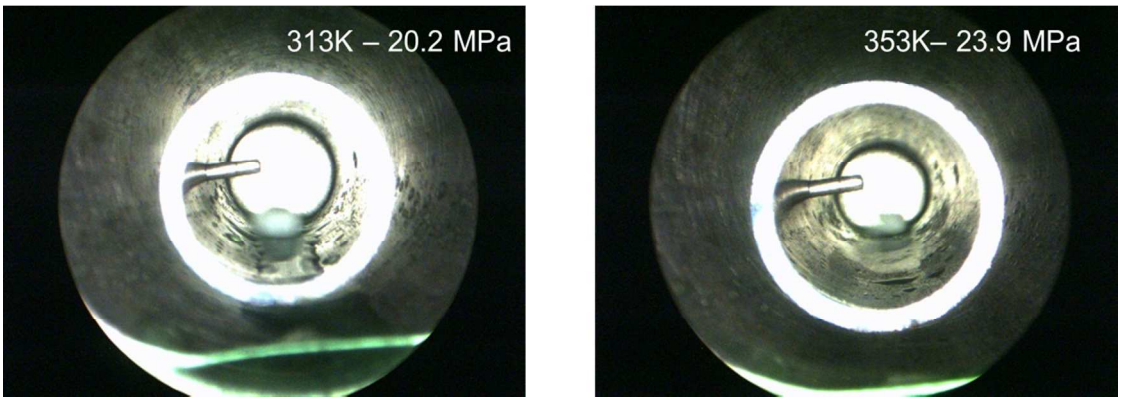

Figure 9. Images from the view cell for a typical experiment at low EtOH concentration showing two phases at pressure conditions much higher than those of the binary system CO_2 + EtOH. The upper phase is rich in CO_2 and EtOH, whilst the lower liquid phase is composed mostly by H_2O and $Ni(NO_3)_2$. The composition of the mixture was: x CO_2= 0.941, x EtOH= 0.057, x $Ni(NO_3)_2 \cdot 6H_2O$ = 1.16 10^{-3}.

For the lower EtOH compositions reported in the table, the aqueous phase was very hard to dissolve and very high solubilisation pressures were required in order to reach single-phase conditions. Depressurization from the single phase led to the appearance of a liquid phase at most conditions. However, it became difficult to distinguish between bubble and dew points. In this region, the solubilisation pressures were much higher than those

found for the CO_2 + EtOH binary system. The low solubility of water in CO_2 increased the equilibrium pressures. In this region, only four compositions were measured at pressures below 30.0 MPa (upper pressure limit of the cell).

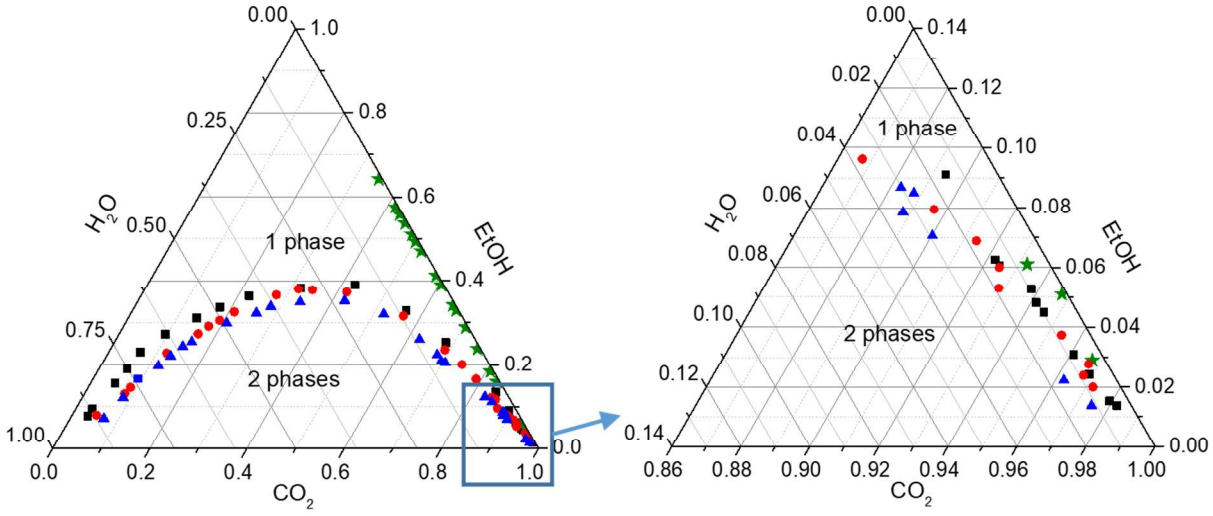

Figure 10. Phase diagram for the CO_2 + EtOH + H_2O ternary system at 313.2 K and different pressures [34]: (■) 10 MPa, (●) 20 MPa and (▲) 30 MPa, and experimental compositions studied for the CO_2 + EtOH + $Ni(NO_3)_2 \cdot 6H_2O$ system at 313.2 K (★). Right image shows an enlargement of the region of lower ethanol concentration. $Ni(NO_3)_2 \cdot 6H_2O$ mole fraction values vary from 1.67 10^{-4} to 1.97 10^{-3} and are given in Table 2.

Figure 10 shows the phase diagram of the ternary system CO_2 + EtOH + H_2O at 313.2 K and 10, 20 and 30 MPa, exhibiting the binodal curves separating the two and one-phase regions together with the experimental compositions studied for the CO_2 + EtOH + $Ni(NO_3)_2 \cdot 6H_2O$ system. The concentration of $Ni(NO_3)_2$ has not been considered in the calculation, whilst the amount of water has been determined from the amount of salt. Enlargement in the region of lower EtOH concentration shows the proximity of the experimental compositions to the binodal line. Although in relation to the binodal curve for

the CO_2 + EtOH + H_2O system most compositions lie in the one phase region, experimentally the larger pressures required for complete solubilisation of the system for compositions poor in ethanol suggests a slight shift of the phase diagram in this region due to the presence of the salt. This effect is more pronounced at high temperature.

To further study the role of water in the system, in one experiment water was removed from the system by adding molecular sieves to the initial $Ni(NO_3)_2 \cdot 6H_2O$ solution. The composition of the mixture was very similar to that shown in Figure 9, which did not lead to one phase. At these conditions, the solubilisation pressure for the salt was lower than that measured without molecular sieves and close to that of the binary system CO_2+ EtOH. At some temperatures, solubilisation pressures were still slightly higher than those of the binary system, which could be due to the incomplete water removal or most likely to the presence of the salt, noticeable in this concentration range.

$Ni(NO_3)_2 \cdot 6H_2O$ can be successfully dissolved in CO_2 + EtOH mixtures. Although the concentration of $Ni(NO_3)_2 \cdot 6H_2O$ in the mixture may seem rather low, large quantities of the nickel salt can be dissolved at very mild conditions, particularly at the large EtOH concentration range. This mixture can be used in metal deposition experiments.

4. Conclusions

$Ni(NO_3)_2 \cdot 6H_2O$ is not soluble in pure CO_2 but can be dissolved in high-pressure CO_2 + ethanol mixtures. Solubility of $Ni(NO_3)_2 \cdot 6H_2O$ in CO_2 + ethanol mixtures was studied at temperatures from (308.2 to 352.2 K) and pressures up to 25 MPa using a view cell. At these temperatures, the solutions were stable and did not decompose. Mole fraction of $Ni(NO_3)_2 \cdot 6H_2O$ varied from 1.67×10^{-4} and 1.97×10^{-3}. At each temperature, for most compositions the phase diagram closely matched that of the binary system CO_2 + EtOH due

to the small concentration of the salt. However, at the lower EtOH concentrations, the presence of water in the compound increased significantly the solubilisation pressures. The Ni concentrations used in these experiments are high enough to perform metal deposition experiments in CO_2. From a practical point of view, in order to solubilise $Ni(NO_3)_2 \cdot 6H_2O$ in CO_2 + ethanol mixtures, it is recommended using EtOH concentrations above 0.1 mole fraction in order to reach complete miscibility at moderate pressures.

Acknowledgements

We gratefully acknowledge the financial support of the Spanish Ministry of Economy and Competitiveness (MINECO), research project CTQ2013-41781-P.

References

1. Beckman, E. J., Supercritical and near-critical CO_2 in green chemical synthesis and processing. *J. Supercrit. Fluids* **2004,** 28, 121–191.

2. Peters, C. J., Multiphase Equlibria in Near-Critical Solvents In *Supercritical Fluids: Fundamentals for Application*, Kiran, E.; LeveltSengers, J. M. H., Eds. 1994; Vol. 273, pp 117-145.

3. de Melo, M. M. R.; Silvestre, A. J. D.; Silva, C. M., Supercritical fluid extraction of vegetable matrices: Applications, trends and future perspectives of a convincing green technology. *J. Supercrit. Fluids* **2014,** 92, 115-176.

4. McHugh, M. A.; Kukronis, V. J., *Supercritical fluid extraction: principles and practice*. 2nd ed.; Butterworth-Heinemann: Stoneham, MA, 1994.

5. Kordikowski, A.; Schenk, A. P.; VanNielen, R. M.; Peters, C. J., Volume expansions and vapor-liquid equilibria of binary mixtures of a variety of polar solvents and certain near-critical solvents. *J. Supercrit. Fluids* **1995,** 8, 205-216.

6. Bozbag, S. E.; Sanli, D.; Erkey, C., Synthesis of nanostructured materials using supercritical CO2: Part II. Chemical transformations. *J. Mater. Sci.* **2012,** 47, 3469-3492.

7. Zhang, Y.; Erkey, C., Preparation of supported metallic nanoparticles using supercritical fluids: A review. *J. Supercrit. Fluids* **2006,** 38, 252-267.

8. Cabañas, A.; Shan, X. Y.; Watkins, J. J., Alcohol-assisted deposition of copper films from supercritical carbon dioxide. *Chem. Mater.* **2003,** 15, 2910-2916.

9. Morley, K. S.; Marr, P. C.; Webb, P. B.; Berry, A. R.; Allison, F. J.; Moldovan, G.; Brown, P. D.; Howdle, S. M., Clean preparation of nanoparticulate metals in porous supports: a supercritical route. *J. Mater. Chem.* **2002,** 12, 1898-1905.

10. Holmes, J. D.; Lyons, D. M.; Ziegler, K. J., Supercritical Fluid Synthesis of Metal and Semiconductor Nanomaterials. *Chem. - Eur. J.* **2003,** 9, 2144-2150.

11. Blackburn, J. M.; Long, D. P.; Cabañas, A.; Watkins, J. J., Deposition of conformal copper and nickel films from supercritical carbon dioxide. *Science* **2001,** 294, 141-145.

12. Castro, A.; Morere, J.; Cabañas, A.; Ferreira, L. P.; Godinho, M.; Ferreira, P.; Vilarinho, P. M., Designing nanocomposites using supercritical CO_2 to insert Ni nanoparticles into the pores of nanopatterned $BaTiO_3$ thin films. *J. Mater. Chem. C* **2017,** 5, 1083-1089.

13. Morère, J.; Royuela, S.; Asensio, G.; Palomino, P.; Enciso, E.; Pando, C.; Cabañas, A., Deposition of Ni nanoparticles onto porous supports using supercritical CO_2: effect of the precursor and reduction methodology. *Philos. Trans. R. Soc., A* **2015,** 373, 1-16.

14. Morère, J.; Sanchez-Miguel, E.; Tenorio, M. J.; Pando, C.; Cabañas, A., Supercritical fluid preparation of Pt, Ru and Ni/graphene nanocomposites and their application as selective catalysts in the partial hydrogenation of limonene. *J. Supercrit. Fluids* **2017,** 120, 7-17.

15. Morère, J.; Tenorio, M. J.; Torralvo, M. J.; Pando, C.; Renuncio, J. A. R.; Cabañas, A., Deposition of Pd into mesoporous silica SBA-15 using supercritical carbon dioxide. *J. Supercrit. Fluids* **2011,** 56, 213-222.

16. Morère, J.; Torralvo, M. J.; Pando, C.; Renuncio, J. A. R.; Cabañas, A., Supercritical fluid deposition of Ru nanoparticles onto SiO_2 SBA-15 as a sustainable method to prepare selective hydrogenation catalysts. *Rsc Adv.* **2015,** 5, 38880-38891.

17. Tenorio, M. J.; Pando, C.; Renuncio, J. A. R.; Stevens, J. G.; Bourne, R. A.; Poliakoff, M.; Cabanas, A., Adsorption of $Pd(hfac)_2$ on mesoporous silica SBA-15 using supercritical CO_2 and its role in the performance of Pd-SiO_2 catalyst. *J. Supercrit. Fluids* **2012,** 69, 21-28.

18. Skerget, M.; Knez, Z.; Knez-Hrncic, M., Solubility of Solids in Sub- and Supercritical Fluids: a Review. *J. Chem. Eng. Data* **2011,** 56, 694-719.

19. Liu, Z., Nanocomposites synthesized using supercritical fluids. *J. Phys.: Conf. Ser.* **1009,** 165, 1-6.

20. Liu, Z. M.; Han, B. X., Synthesis of Carbon-Nanotube Composites Using Supercritical Fluids and Their Potential Applications. *Adv. Mater.* **2009,** 21, 825-829.

21. Ming, J.; Wu, C.; Cheng, H.; Yu, Y.; Zhao, F., Reaction of hydrous inorganic metal salts in CO_2 expanded ethanol: Fabrication of nanostructured materials via supercritical technology. *J. Supercrit. Fluids* **2011,** 57, 137-142.

22. Perez, E.; Cabañas, A.; Renuncio, J. A. R.; Sanchez-Vicente, Y.; Pando, C., Cosolvent Effect of Methanol and Acetic Acid on Dibenzofuran Solubility in Supercritical Carbon Dioxide. *J. Chem. Eng. Data* **2008,** 53, 2649-2653.

23. Perez, E.; Cabañas, A.; Sanchez-Vicente, Y.; Renuncio, J. A. R.; Pando, C., High-pressure phase equilibria for the binary system carbon dioxide plus dibenzofuran. *J. Supercrit. Fluids* **2008,** 46, 238-244.

24. Morère, J.; Tenorio, M. J.; Pando, C.; Renuncio, J. A. R.; Cabañas, A., Solubility of two metal-organic ruthenium precursors in supercritical CO_2 and their application in supercritical fluid technology. *J. Chem. Thermodyn.* **2013,** 58, 55-61.

25. Tenorio, M. J.; Cabañas, A.; Pando, C.; Renuncio, J. A. R., Solubility of $Pd(hfac)_2$ and $Ni(hfac)_2{\cdot}2H_2O$ in supercritical carbon dioxide pure and modified with ethanol. *J. Supercrit. Fluids* **2010,** 70, 106-111.

26. Chin, H. Y.; Lee, M. J.; Lin, H. M., Vapor-Liquid Phase Boundaries of Binary Mixtures of Carbon Dioxide with Ethanol and Acetone. *J. Chem. Eng. Data* **2008,** 53, 2393-2402.

27. Tanaka, H.; Kato, M., Vapor-Liquid-Equilibirum Properties of Carbon-Dioxide plus Ethanol Mixture at High-Pressures. *J. Chem. Eng. Jpn.* **1995,** 28, 263-266.

28. Chen, H.-I.; Chang, H.-Y.; Huang, E. T. S.; Huang, T.-C., A New Phase Behavior Apparatus for Supercritical Fluid Extraction Study. *Ind. Eng. Chem. Res.* **2000,** 39, 4849-4852.

29. Joung, S. N.; Yoo, C. W.; Shin, H. Y.; Kim, S. Y.; Yoo, K. P.; Lee, C. S.; Huh, W. S., Measurements and correlation of high-pressure VLE of binary CO_2-alcohol systems (methanol, ethanol, 2-methoxyethanol and 2-ethoxyethanol). *Fluid Phase Equilib.* **2001,** 185, 219-230.

30. Suzuki, K.; Sue, H., Isothermal Vapor-Liquid-Equilibrium Data for Binary Systems at High Pressures- Carbon Dioxide + Methanol, Carbon Dioxide + Etanol, Carbon Dioxide + 1-Propanol, Methane+ Ethanol, Methane+ 1-Propano+, Ethane + Ethanol and Etane -1-Propanol Systems. *J. Chem. Eng. Data* **1990,** 35, 63-66.

31. Knez, Z.; Skerget, M.; Ilic, L.; Lutge, C., Vapor-liquid equilibrium of binary CO_2-organic solvent systems (ethanol, tetrahydrofuran, ortho-xylene, meta-xylene, para-xylene). *J. Supercrit. Fluids* **2008,** 43, 383-389.

32. Secuianu, C.; Feroiu, V.; Geana, D., Phase behavior for carbon dioxide plus ethanol system: Experimental measurements and modeling with a cubic equation of state. *J. Supercrit. Fluids* **2008,** 47, 109-116.

33. Wu, W. Z.; Ke, J.; Poliakoff, M., Phase boundaries of CO_2 plus toluene, CO_2 plus acetone, and CO_2 plus ethanol at high temperatures and high pressures. *J. Chem. Eng. Data* **2006,** 51, 1398-1403.

34. Durling, N. E.; Catchpole, O. J.; Tallon, S. J.; Grey, J. B., Measurement and modelling of the ternary phase equilibria for high pressure carbon dioxide-ethanol-water mixtures. *Fluid Phase Equilib.* **2007,** 252, 103-113.

FOR TABLE OF CONTENTS ONLY